Hydraulics Research
Wallingford

THE RELATIVE CONTRIBUTIONS OF WAVES AND TIDAL CURRENTS TO MARINE SEDIMENT TRANSPORT

R L Soulsby

Report No SR 125
April 1987

Registered Office: Hydraulics Research Limited, Wallingford, Oxfordshire OX10 8BA.
Telephone: 0491 35381. Telex: 848552

This report describes work carried out by Hydraulics Research into the movement of sand by combined waves and currents. It has been funded by the Ministry of Agriculture, Fisheries and Food under contract number CSA 992, the nominated officer being Mr A Allison. At the time of report the Hydraulics Research nominated officer was Dr S W Huntington.

The report is published on behalf of the Ministry of Agriculture, Fisheries and Food, but any opinions expressed within it are those of the authors only, and are not necessarily of the ministry who sponsored the research.

ABSTRACT

In many tidal sea areas the long-term mean sediment transport is the resultant of a wide range of different combinations of wave and tidal current conditions occurring during the course of a year, from calm conditions during neap tides to extreme events of major storms coupled with spring tides. It is shown, using wave and current data from the North Sea, that the most important contributions to the long-term transport are made by fairly large but not too infrequent waves, combined with tidal currents lying between the mean neap and spring maxima. Weak currents and low waves make small contributions because, although they occur very frequently, their potential for sediment transport is small. Equally the most extreme events do not make large contributions because, although they have a large potential for sediment transport, they occur too infrequently. As the wave climate becomes effectively weaker, due for example to increasing the water depth, the important events shift to smaller wave-heights and larger currents.

CONTENTS

1 INTRODUCTION

In many areas of coastal and shelf seas the most significant sediment transport occurs under the combined action of waves and tidal currents. In essence, the waves act as a very effective stirring agent to mobilise the sediment, while the currents are necessary to transport it.

In recent years effort has focussed on understanding the physics of the boundary-layer processes under combined waves and currents in order to provide improved sediment transport formulae for such conditions. But at any chosen site where sediment transport predictions are required a large number of combinations of wave and current conditions will occur during the course of a year, ranging from calm conditions coupled with neap tides to major storms coupled with spring tides. Thus, even if a perfectly accurate sediment transport formula were available, there is difficulty in deciding which wave and current conditions should be applied as inputs in order to provide an estimate of the long term transport. This prompts us to investigate the relative importance, over a long period of time, of currents and waves as agents for sediment transport.

It is often said that sediment transport is dominated by extreme events, that is, spring tides and/or major storms. But since extreme events are very infrequent, it is not clear whether their contributions to the long-term transport will be more or less important than those provided by a succession of weaker, but very frequent, events. Since the effect of waves at the sea bed is attenuated by the water depth, the answers to the above questions will depend on the water depth, as well as on the prevailing current and wave height/period conditions.

These questions are addressed here, using for reference a particularly high quality set of wave and current measurements at a site in the North Sea, but providing answers which it is believed will be typical of many seas with strong tidal currents and significant wave action.

The principles of the Hydraulics Research computer programs ORBVEL and EXTREMSED which perform the calculations are also illustrated.

2 FORMULATION

To examine the above questions it is necessary to work in terms of the probabilities of occurrence of current and wave conditions at a given site. The probability distributions for the currents and waves separately

are assumed to be derived from long (eg several years) series of measurements, with each measurement taken over a time interval which is long compared with a turbulence time-scale or a wave period but short compared with a tidal period (eg 10 to 60 minutes). We take no account here of the directions of either the currents or the waves, since we are primarily interested in the amount of sediment transport activity contributed by a particular current and wave condition, irrespective of the direction of transport. Of course, in a real practical problem the directions of transport will often be a decisive factor.

We assume that the effect of a current on sediment transport can be characterised by its depth-averaged speed U. A discrete probability distribution $p_c(U_i)$ for U is then defined by dividing the U axis into equal intervals, with U_i being the speed at the centre of the ith interval, and where $\sum_i p_c(U_i) = 1$. The effect of waves on sediment transport is assumed to be characterised by W, the rms near-bottom wave orbital velocity. The discrete probability distribution $p_w(W_j)$ for W is defined analogously to $p_c(U_i)$, with W_j being the value of W at the centre of the jth interval, and $\sum_j p_w(W_j) = 1$. The widths of the intervals for U and W are not necessarily equal.

Consider firstly the case when waves are negligible, as for example occurs in a river. Then the current-only sediment transport rate Q_c is a function only of U, assuming that other parameters such as water depth and sediment grain size are held constant. The long-term mean sediment transport rate, $\langle Q_c \rangle$ is given by:

$$\langle Q_c \rangle = \sum_i p_c(U_i)\, Q_c(U_i), \qquad (1)$$

and the proportion S_c of $\langle Q_c \rangle$ which is contributed by current speeds in the interval centred on U_i is:

$$S_c(U_i) = \frac{p_c(U_i)\, Q_c(U_i)}{\langle Q_c \rangle} \qquad (2)$$

Turning now to the combined current and wave case we must calculate the joint probability p_{cw} of obtaining a current speed in the interval centred on U_i simultaneously with a wave whose rms orbital velocity lies in the interval centred on W_j. In the general case where the currents are partly tidal and partly wind induced, and the waves are due partly to swell from distant parts and partly to local winds, it will

be difficult to calculate the joint probability distribution. However, in many sea areas the current is predominantly due to tidal (and hence astronomical) forcing, while the waves are predominantly due to meteorological forcing. Under these conditions the currents and waves can be assumed to act independently, and the joint probability is:

$$p_{cw}(U_i, W_j) = p_c(U_i)\, p_w(W_j) \qquad (3)$$

Suppose that the sediment transport rate which results from a combination of a current U with waves of orbital velocity W is $Q_{cw}(U, W)$, where other parameters such as grain size and water depth are held fixed. Then the long-term mean sediment transport rate is:

$$\langle Q_{cw} \rangle = \sum_i \sum_j p_{cw}(U_i, W_j)\, Q_{cw}(U_i, W_j) \qquad (4)$$

The proportion S_{cw} of the long-term mean sediment transport which is contributed by a combination of current U_i and waves W_j is thus:

$$S_{cw}(U_i, W_j) = \frac{p_{cw}(U_i, W_j)\, Q_{cw}(U_i, W_j)}{\langle Q_{cw} \rangle} \qquad (5)$$

Our aim is to investigate how S_{cw} varies with U and W, and also how the distribution of S_{cw} varies with the water depth h.

3 RESULTS

A purely synthetic example is taken as an illustration, with the wave and current data measured at different (though not widely separated) sites, and using an arbitrary water depth and sediment size. The data sets were chosen from the literature for their high quality and long duration, and the depths and sediment type (sand) chosen so as to give sediment transport under a wide range of conditions. Both data sets were obtained in the North Sea off the east coast of England.

The current data set was measured at the Inner Dowsing Light Tower using an Aanderaa current meter mounted 14m above the sea bed in a mean depth of 20m (Pugh, 1982). For the present illustrative purposes these values are treated as representing the depth-mean current. The measurements extended over one year and were recorded every 10 minutes, subsequently filtered to hourly mean values. The probability distribution $p_c(U_i)$ for intervals of $0.1 ms^{-1}$ shown in Fig 1 of this

report is based on Fig 1 of Pugh (1982), extended to extreme values by using his Fig 3. The velocity amplitudes of mean neap and mean spring tides at this site are 0.45 and 0.93ms^{-1} respectively (Pugh and Vassie, 1976). Because the tidal ellipse at this site is relatively open there are no occurrences of U in the interval 0 to 0.1ms^{-1}. The frequency of occurrence reaches a peak slightly below the maximum speed of mean neap tides, decreases towards the maximum speed of mean spring tides, and tails off rapidly for larger speeds corresponding to the largest spring tides possibly superimposed by surge currents.

One of the simplest forms of current only sediment transport formula in use is a power law of the form:

$$Q_c(U) = \alpha U^n \qquad (6)$$

where the coefficient α has suitable dimensions, and may be a function of water-depth, sediment grain-size and density, etc. Taking as an example $n = 4$ and $\alpha = 1380 gs^3 m^{-5}$ (see later), the long-term mean sediment transport rate obtained by using Eq (6) in Eq (1) is $\langle Q_c \rangle = 245 gs^{-1} m^{-1}$. The distribution $S_c(U_i)$ of contributions to $\langle Q_c \rangle$ obtained from Eq (2) is shown in Fig 1. The largest contributions are made by currents with speeds close to the peak speed of mean spring tides, with relatively small contributions made by the most extreme current speeds.

The wave data set for the present example was measured at the Outer Dowsing Light Vessel in a mean depth of 26m using a shipborne wave recorder (Fortnum, 1981). The measurements used here were taken over three complete years, with 12 minute records taken every 3 hours. Since the wave data is presented in terms of surface elevation it is necessary to convert it to bottom orbital velocities before $p_w(W_j)$ can be obtained. Fortnum (1981, Fig 3.5.1.5) presents a scatter plot of the number of occurrences during the three years of waves with significant height H_s and zero-crossing period T_z divided into 0.5m intervals of H_s and 0.5s intervals of T_z, shown here in Fig 2. The simplest means of calculating W would be to assume that each entry on the scatter plot corresponds to a monochromatic wave of height H_s and period T_z, for which the near-bottom orbital velocity amplitude could be obtained by linear wave theory. However, in reality each H_s and T_z corresponds to a spectrum of waves, each frequency of which will have a different attenuation with depth. It was shown by Soulsby and Smallman (1986) and Soulsby (1987) that, using linear wave theory at each frequency, and assuming the waves

have a JONSWAP spectrum defined by the two parameters H_s and T_z, the rms near-bottom orbital velocity W can be presented as a single curve which is a function of $t = (h/g\ T_z^{\,2})^{\frac{1}{2}}$. For $0 < t < 0.55$, the curve is approximated to better than ±1.0% by the expression:

$$\frac{W}{H_s}\left(\frac{h}{g}\right)^{\frac{1}{2}} = \frac{0.25}{(1+At^2)^3} \qquad (7)$$

where:

$$A = \left[6500 + (0.56 + 15.54t)^6\right]^{1/6}, \qquad (8)$$

h is the water depth, and g is the acceleration due to gravity. A water depth of 10m is chosen for the first illustration, which will allow the wave action to reach the bottom without undue attention. Applying Eq (7) to each combination of H_s and T_z in the scatter plot, yielded the values of W shown superimposed as contours in Fig 2. The number of occurrences falling into each $0.1ms^{-1}$ interval of W were then totalled and divided by the total number of records to yield the probability distribution $p_w(W_j)$ shown in Fig 3. The maximum frequency of occurrence lies in the interval 0.1 to $0.2ms^{-1}$, decreasing relatively smoothly as W increases. The largest recorded values of W lie between 1.3 and $1.4ms^{-1}$, having a probability of 0.043%.

The conversion of an H_s-T_z scatter plot to the probability distribution of W is undertaken by the Hydraulics Research computer program ORBVEL.

The joint probability $p_{cw}(U_i, W_j)$ obtained by combining $p_c(U_i)$ and $p_w(W_j)$ using Eq (3), shown in Fig 4, decreases rapidly for simultaneous increases in U and W. The most frequently occurring combination of U and W in the table occurs nearly 40 million times more often than the least common combination.

As a combined wave-and-current sediment transport formula we use that derived by Grass (1981), namely:

$$Q_{cw}(U, W) = \alpha U^n \left[1+\beta\left(\frac{W}{U}\right)^2\right]^{\left(\frac{n-1}{2}\right)} \qquad (9)$$

The values of the coefficients α and n are chosen by matching the formula in its currents-only limit (W=0), given by Eq (6), either to field data or to a selected currents-only formula from the wide range available. Using the field data of Owen and Thorn (1978) measured in 2.5 to 7m of water over a sand bed, Grass obtained values of the constants: α = 1380 (for U and W in

ms^{-1}, Q_{cw} in $g\ s^{-1}m^{-1}$), n = 4. For the coefficient β he obtained $\beta = 0.08/C_D$, where C_D is the drag coefficient defined by (bed shear stress) = $\rho C_D U^2$. If the velocity profile is logarithmic throughout the depth with a bed roughness length z_o, then:

$$C_D = \left[\frac{\kappa}{\ln(h/z_o)-1}\right]^2 \qquad (10)$$

where $\kappa = 0.4$ is von Karman's constant, and a typical roughness for a rippled sand bed is $z_o = 0.6cm$ (Soulsby, 1983).

The Grass formula was selected for the present purposes more for its simplicity and versatility than for accuracy. However, a comparison by Bettess (1985) of several wave-and-current sediment transport formulae (but not including Eq (9)) with laboratory and field data showed that even the best of them could predict Q_{cw} to within a factor of 10 only 50% of the time. Thus there is little reason to choose any other formula in preference to that of Grass.

For a depth h = 10m and $z_o = 0.6cm$, Eq (10) yields $C_D = 3.9 \times 10^{-3}$ and hence $\beta = 20.6$. Using this value of β and Grass's values of α and n in Eq (9), and substituting into it all the possible combinations of U and W, gives the variation of Q_{cw} with U and W shown in Fig 5. The value of Q_{cw} increases rapidly with increases in both U and W. The largest value of Q_{cw} in the table is almost 700 thousand times larger than the smallest.

In broad terms the probability p_{cw} of occurrence of a particular combination of U_i and W_j decreases rapidly from bottom left to top right of Fig 4. Conversely the transport rate Q_{cw} produced by that combination increases rapidly from bottom left to top right of Fig 5. Since the long-term contribution made by a combination of U_i and W_j to the long-term mean transport is given by the product of the appropriate entry in Fig 4 with the corresponding entry in Fig 5, the answers to our original questions will depend on a fine balance between these two opposing trends.

Performing the product for each entry and summing all the entries, as indicated by Eq (4), yields $\langle Q_{cw} \rangle = 3.0 \times 10^3 g\ s^{-1}m^{-1}$ for the present example. This is more than 10 times larger than the value $\langle Q_c \rangle = 245 gs^{-1}m^{-1}$ obtained if waves are neglected.

The table of the individual products is then normalised by $\langle Q_{cw} \rangle$ according to Eq (5) to give the

contribution S_{cw} in parts per thousand of each combination of U_i and W_j to the long-term transport (Fig 6). We see that the largest contributions (>10ppt) are produced by fairly large but not too infrequent waves, combined with currents lying roughly between the mean neap and spring maxima. These contributions added together provide almost half (49%) of the overall transport. The largest observed waves provide small but non-negligible contributions (up to 3ppt), and for a more complete picture it would be necessary to extend $p_w(W_j)$ to more extreme values as was done for $p_c(U_i)$. Contributions < 1ppt are shown blank in Fig 6. If all the contributions < 1ppt in the table are added, their total provides only 2.5% of the overall transport. This total is not likely to be increased greatly by the additional values which extend beyond the range of the table. It is evident that very weak currents and low waves provide only small contributions to the long-term mean, because, although they occur frequently, their potential for sediment transport is small. However, it is equally evident that combinations of the very largest waves and currents do not provide large contributions, because, although they have a large potential for transport, they occur very infrequently. That is, the most extreme events do not dominate in the long term. As an aid to interpretation, scales of $\overline{H_s}$ and $\overline{T_z}$ are included on the waves axis, these being the mean values of H_s and T_z for all the occurrences in each interval of W. The most important waves for sediment transport in this example are seen to be those with heights:

$1.3 < H_s < 4.0$m and $5.3 < T_z < 7.3$s.

Similar calculations have been performed using the same basic data sets, but using water depths of h=5, 20 and 50m in the wave orbital velocity calculations. The values of C_D and hence β were also adjusted accordingly (Eq 10). The results are summarised in Fig 7, where only large (>10ppt), medium (1 to 10ppt), and small (<1ppt) contributions are identified. Note that the ordinate on these figures is linear in W, though for intercomparison purposes the irregular scale in $\overline{H_s}$ is more useful. The results are indicative only, since the same H_s-T_z scatter plot was used at all depths without any allowance for wave-breaking, so that the larger values of H_s are unrealistically large for h=5 and 10m. The patterns for h=5 and 10m are similar, but as the depth increases from 10 to 50m the important contributions are provided by progressively less high waves and

larger currents. As wave effects become even weaker the distribution of S_{cw} tends to the current-only distribution S_c shown in Fig 1.

The calculation of $< Q_{cw} >$ and $S_{cw}(V_i, W_j)$ from $p_c(V_i)$ and $p_w(W_j)$ is undertaken by the Hydraulics Research computer program EXTREMSED.

4 DISCUSSION

The importances or otherwise of extreme currents and waves for long-term sediment transport depends on the rate of decay with respect to U and W of the product $p_{cw}(U_i, W_j)\, Q_{cw}(U_i, W_j)$. Since, as we have seen, there is a rather fine balance between the rates of decrease of p_{cw} and increase of Q_{cw}, small changes in the form of either of these quantities could possibly have a large effect on the distribution $S_{cw}(U_i, W_j)$. Sensitivity to these forms is now investigated.

Various authors have suggested formulae for the sediment transport rate Q_{cw} under combined waves and currents, some of which were reviewed by Bettess (1985). The dependence of many of these on U and W is broadly similar, and can to some extent be simulated by varying the values of the constants β and n in the Grass formula, Eq (9). Because of the normalisation in Eq (5), the value of S_{cw} does not depend on the constant α. Several currents-only sediment transport formula have a dependence $Q_c \sim U^3$ at large velocities (Dyer, 1986) corresponding to n=3, while the Engelund and Hansen (1967) formula, which is widely regarded as one of the more reliable currents-only formulae, corresponds to n=5. Taking the Dowsing data with h=10m, β=20.6 and n=4 as the "standard" values, the value of n was therefore varied to 3 and 5 (Fig 8a). As n increases from 3 to 5 the important contributions to S_{cw} are provided by progressively larger (and more infrequent) wave-heights, but the range of important current speeds is relatively unchanged. In cases where the effect of waves is relatively unimportant (eg h=50m, Fig 7), one would expect the important contributions to be made by progressively larger current speeds as n increases.

The wave-and-current sediment transport formula of Bijker (1967) used effectively a value of $\beta = 0.324/C_D$, while Swart (1974) used $\beta = 0.5 f_w/C_D$ where the wave friction factor f_w takes values typically in the range 0.002 to 0.3. Again taking the Dowsing data with h=10m, $\beta = 0.08/C_D$=20.6 and n=4 as the standard values, the value of β was varied to $0.04/C_D$ = 10.3 and $0.12/C_D$ = 30.9 (Fig 8b). As β increases from 10.3 to 30.9 the important contributions to S_{cw} are provided

by progressively larger wave-heights, but the dependence is weaker than that on n.

The Grass formula, in common with some of the other wave-and-current formulae, does not incorporate a threshold of motion criterion. If such a threshold were incorporated, as might be required for transport of gravel for example, then one might expect extreme events to become relatively more important.

Perhaps the most critical assumption made in the present formulation is that of the independence of U and W used in Eq (3). While this is a fairly good assumption for areas with dominant tidal currents such as much of the Northwest European shelf, it will not be valid in areas where wind-induced or surge currents dominate, such as the northern North Sea and much of the North American shelf. It will also not be valid in the surf zone where wave-induced alongshore currents dominate. Even in tidally dominated areas the most extreme currents will have a wind-induced component. If U and W are partially correlated, their joint probabilities become much larger for extreme events, so that the distribution of S_{cw} becomes more biassed towards extreme events. If both U and W are functions of the wind speed only, then they are completely correlated and the distribution of S_{cw} is related to the probability distribution for wind speed in a manner analogous to Fig 1, but with wind speed replacing current speed. Ideally one would hope to obtain simultaneous long data-sets of U and W so that the joint probabilities could be calculated directly and the resulting distribution of S_{cw} could be constructed.

Only one data set each of waves and currents has been used, and to increase the generality of the results it would be desirable to use a number of different representative examples. However, to some extent the effect of different data sets has been simulated by varying the water depths (Fig 7) and the coefficient β (Fig 8). A decrease in h or an increase in β has a similar effect to an increase in the severity of the wave conditions relative to the currents. Similarly variations in the sediment grain-size have been simulated by varying the coefficients α and n. It was seen that none of these variations changed the conclusions qualitatively.

5 SUMMARY

The contributions to long-term sediment transport by different combinations of waves and currents have been calculated, using as an illustration high quality data-sets from the North Sea. Both currents and waves

were found to have important roles, with waves enhancing the mean transport by a factor of more than 10 compared with transport in the absence of waves. The largest contributions were provided by fairly large but not infrequent waves, superimposed on currents lying roughly between the peak speeds of mean neap and mean spring tides. Very strong currents and very large waves were found not to make significant contributions; that is, the long term transport is not dominated by extreme events as had sometimes been surmised.

As water depth was increased, the important contributions were made by more extreme currents combined with less extreme wave-heights. The results, while holding generally in broad terms, were fairly sensitive to the form of sediment transport relation used, because of the fine balance between the increase in transport rate and the decrease in frequency of occurrence as wave and current conditions become more severe. The above results apply to sea areas in which the currents are dominantly tidal, and the sediment is sand. In areas with dominant wind or wave induced currents, or for gravel where threshold effects are important, a greater contribution to long term sediment transport from extreme events is expected.

6 ACKNOWLEDGEMENTS

I am indebted to Dr P J Hawkes and Mr N Oliver for their assistance with the computing.

7 REFERENCES

1. Bettess R, 1985. Sediment transport under waves and currents. Hydraulics Research Report SR 22.

2. Bijker E W, 1967. Some considerations about scales for coastal models with movable bed. Delft Hydraulics Laboratory, Pub No 50.

3. Dyer K R, 1986. Coastal and estuarine sediment dynamics. John Wiley, Chichester, 342pp.

4. Engelund F and Hansen E, 1967. A monograph on sediment transport in alluvial streams. Teknisk Forlag, Copenhagen.

5. Fortnum B C H, 1981. Waves recorded at Dowsing Light Vessel between 1970 and 1979. Institute of Oceanographic Sciences Report No 126.

6. Grass A J, 1981. Sediment transport by waves and currents. SERC London Centre for Marine Technology Report No FL29.

7. Owen M W and Thorn M F C, 1978. Effect of waves on sand transport by currents. Proc 16th Coastal Eng Conf, Hamburg, pp1675-1687.

8. Pugh D T, 1982. Estimating extreme currents by combining tidal and surge probabilities. Ocean Eng, 9 (4), pp361-372.

9. Pugh D T and Vassie J M, 1976. Tide and surge propagation offshore in the Dowsing region of the North Sea. Deutsche Hydrographische Zeitschrift, 29, pp163-213.

10. Soulsby R L, 1983. The bottom boundary layer of shelf seas. In: Physical Oceanography of Coastal and Shelf Seas, B Johns (Ed), Elsevier, Amsterdam, pp189-266.

11. Soulsby R L, 1987. Calculating bottom orbital velocity beneath waves. Submitted to Coastal Engineering.

12. Soulsby R L and Smallman J V, 1986. A direct method of calculating bottom orbital velocity under waves. Hydraulics Research Report SR 76.

13. Swart D H, 1974. Offshore sediment transport and equilibrium beach profiles. Delft Hydraulics Laboratory Pub No 131.

Figures

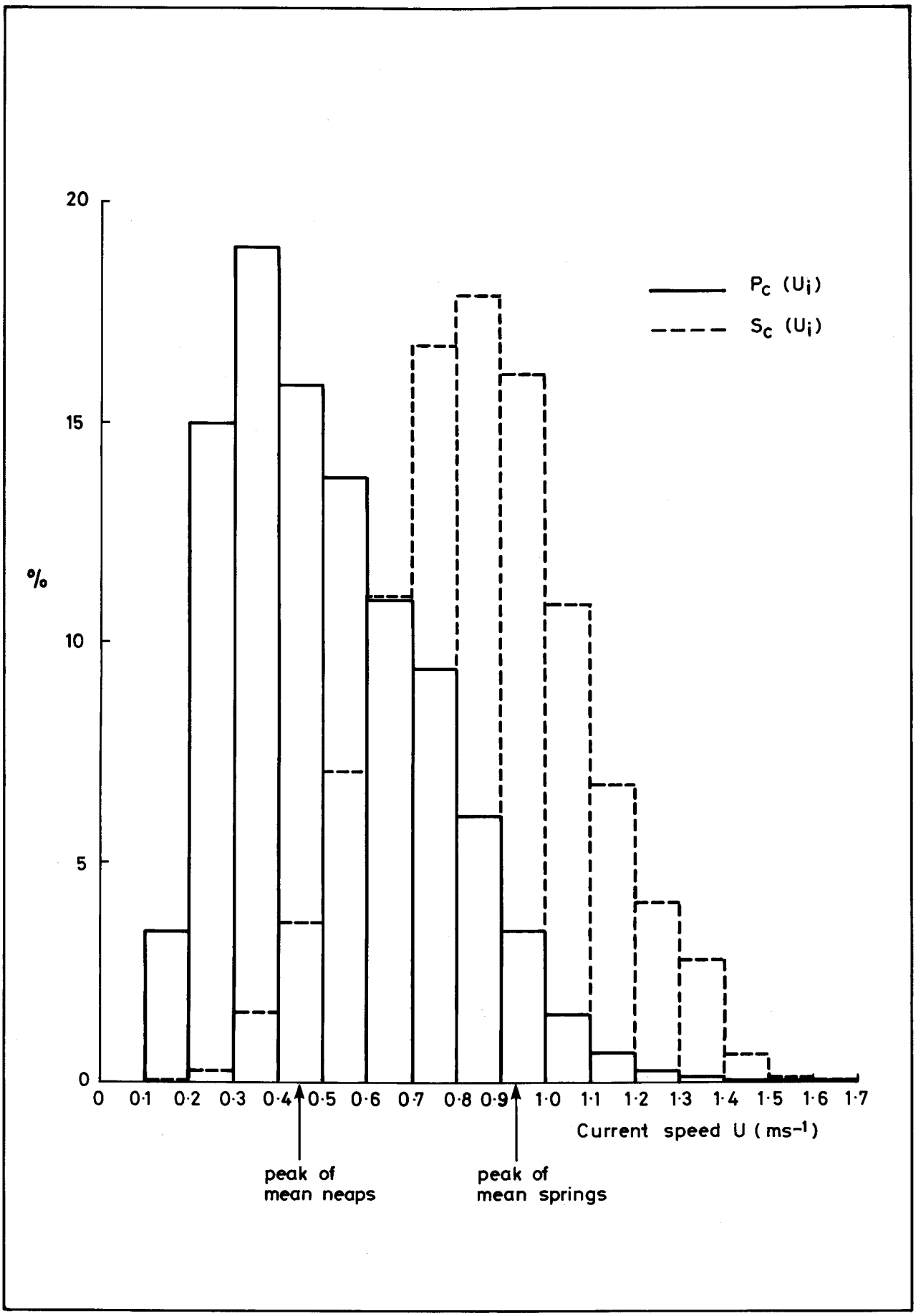

Fig 1 Probability distribution $p_c(U_i)$ of current speed at Inner Dowsing (Pugh, 1982), and the corresponding fractional contribution $S_c(U_i)$ to the long-term sediment transport

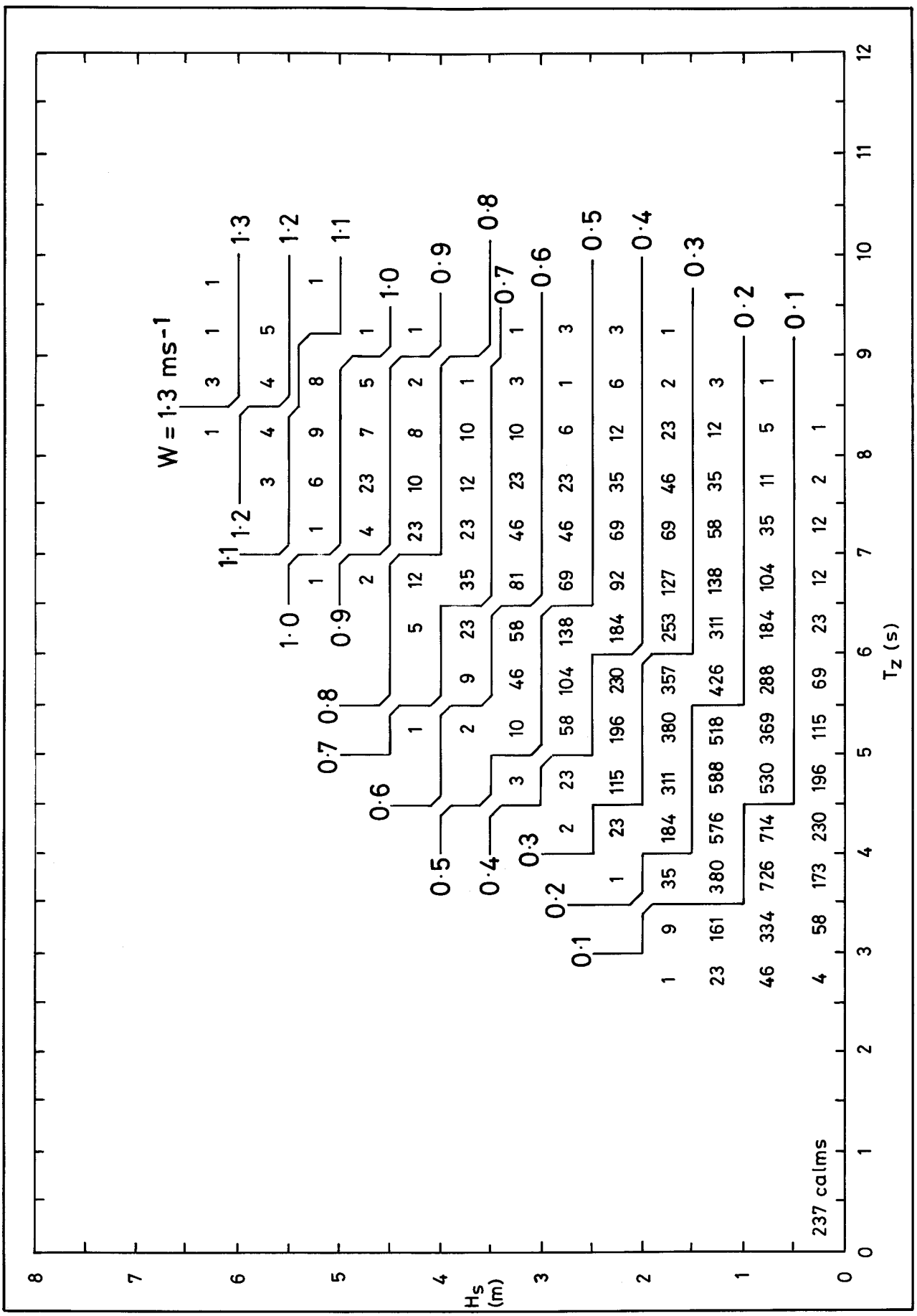

Fig 2 H_s-T_z scatter plot for waves measured at Outer Dowsing (Fortnum, 1981), showing number of occurrences in each interval out of a total of 11293 observations. The rms bottom orbital velocity W obtained from Eq (7) with h=10m is superimposed as contours in ms^{-1}

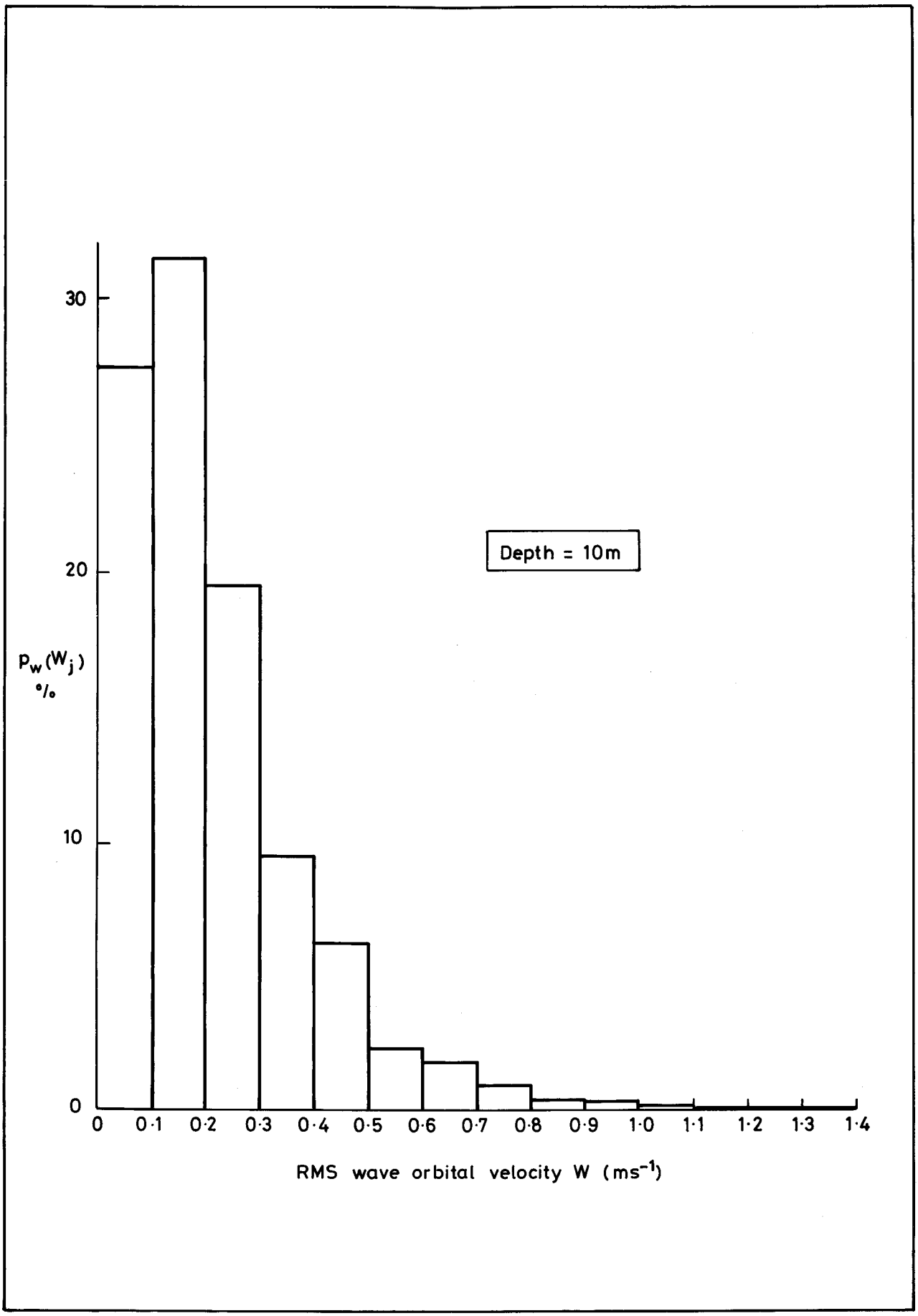

Fig 3 Probability distribution $p_w(W_j)$ of rms bottom orbital velocity for h=10m at Outer Dowsing

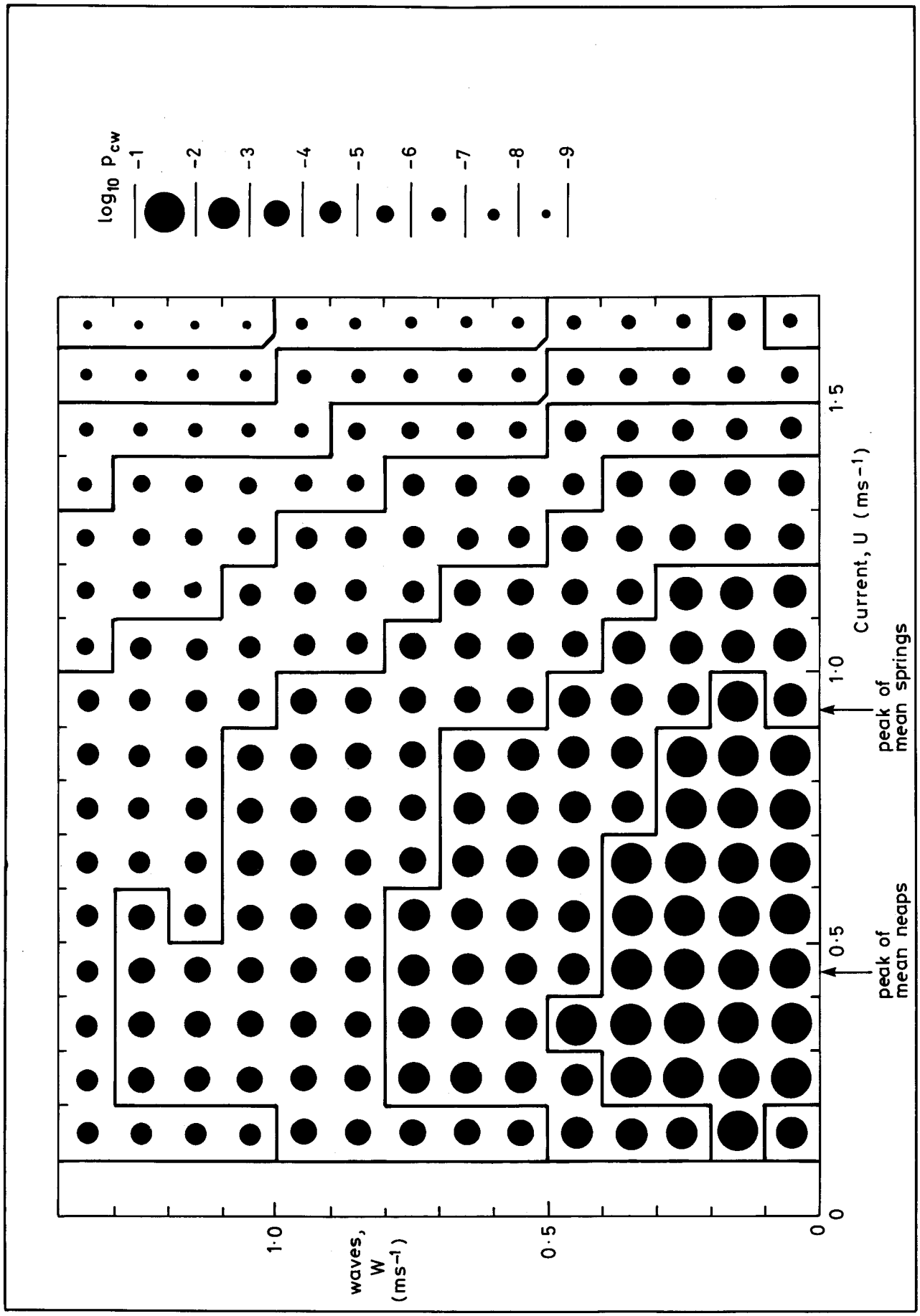

Fig 4 Joint probability distribution $p_{cw}(U_i, W_j)$ of simultaneous occurrence of current and wave velocities from Eq (3) for the Dowsing data with h=10m

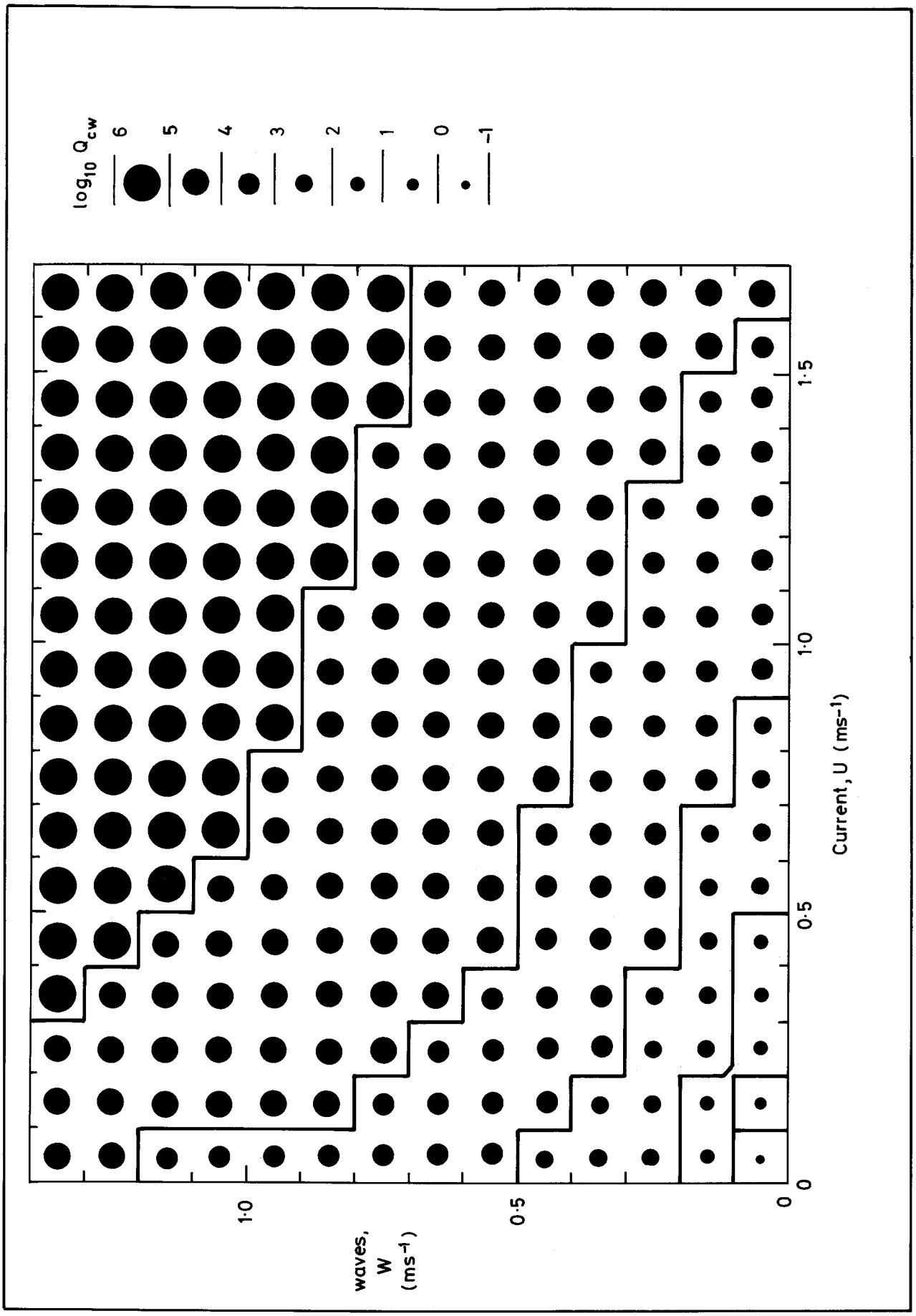

Fig 5 Sediment transport rate $Q_{cw}(U_i, W_j)$ in $gs^{-1}m^{-1}$ due to combined waves and currents using Eq (9) with $\alpha = 1380 gs^{3}m^{-5}$, $\beta = 20.6$ and $n = 4$

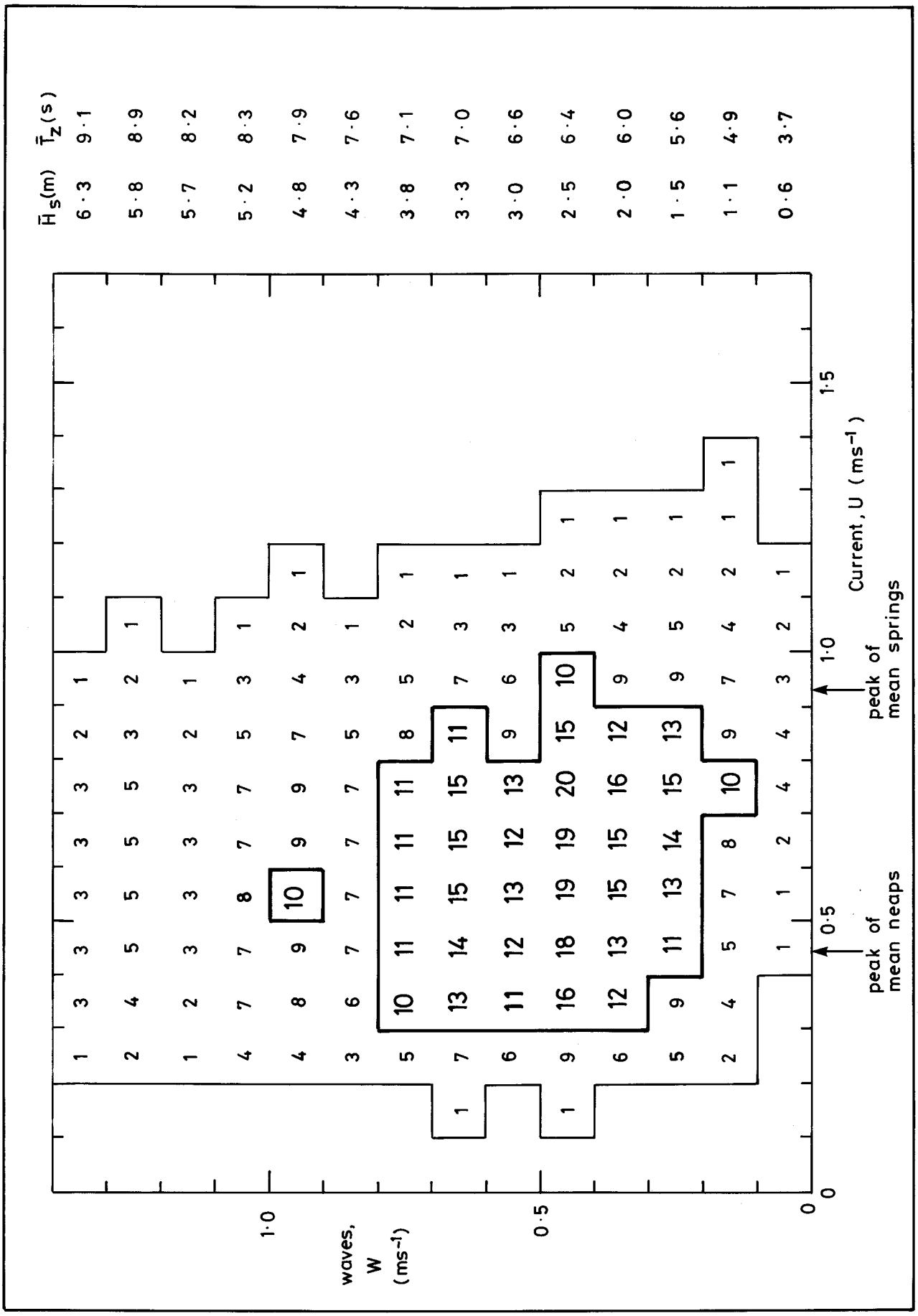

Fig 6 Contributions $S_{cw}(U_i, W_j)$ in ppt made by combined waves and currents to the long-term mean sediment transport for the Dowsing data and the Grass formula, for h=10m, α=1380gs $^3m^{-5}$, β=20.6, n=4. Values <1ppt are not shown

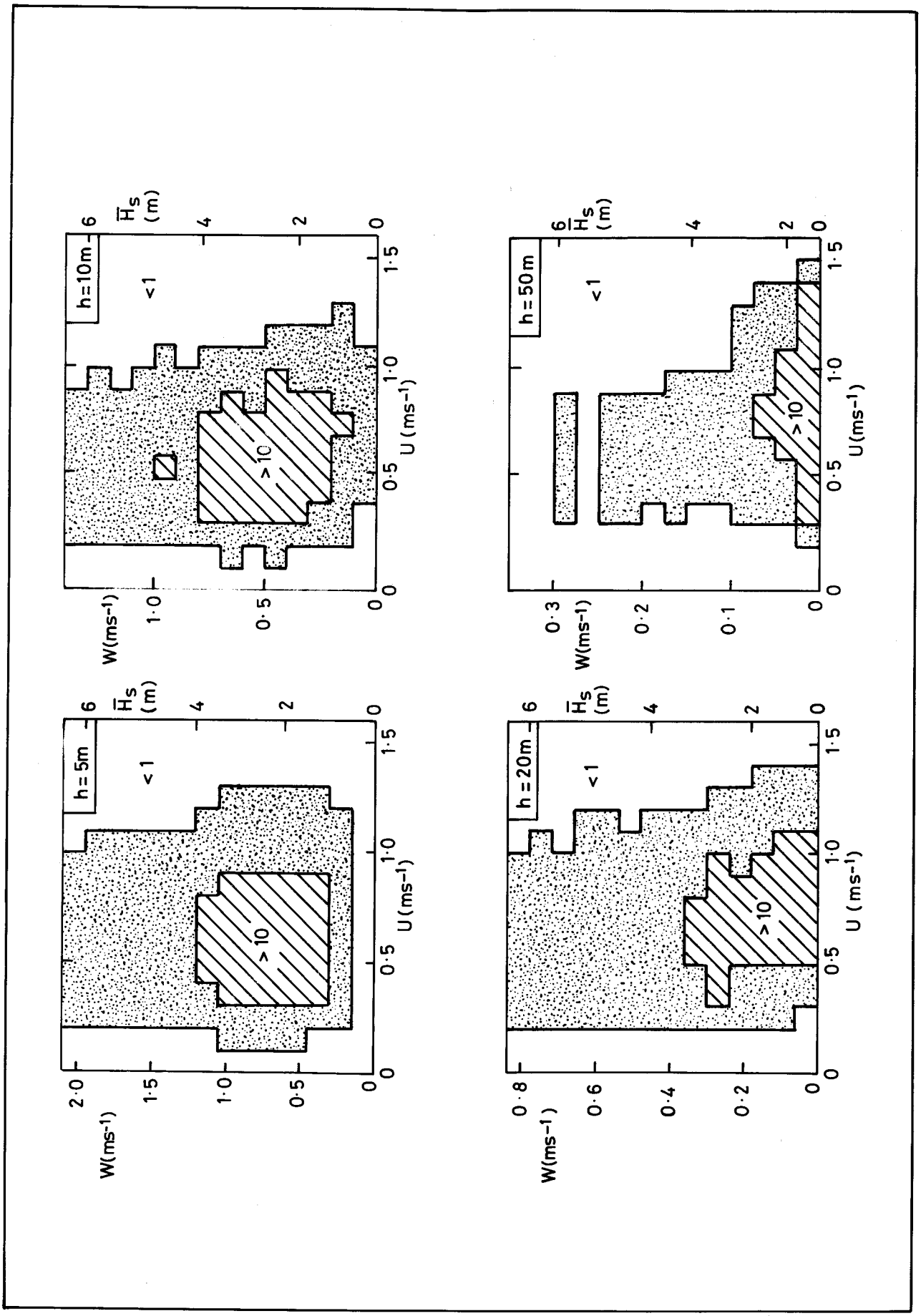

Fig 7 Variation with water depth h of the distribution $S_{cw}(U_i, W_j)$

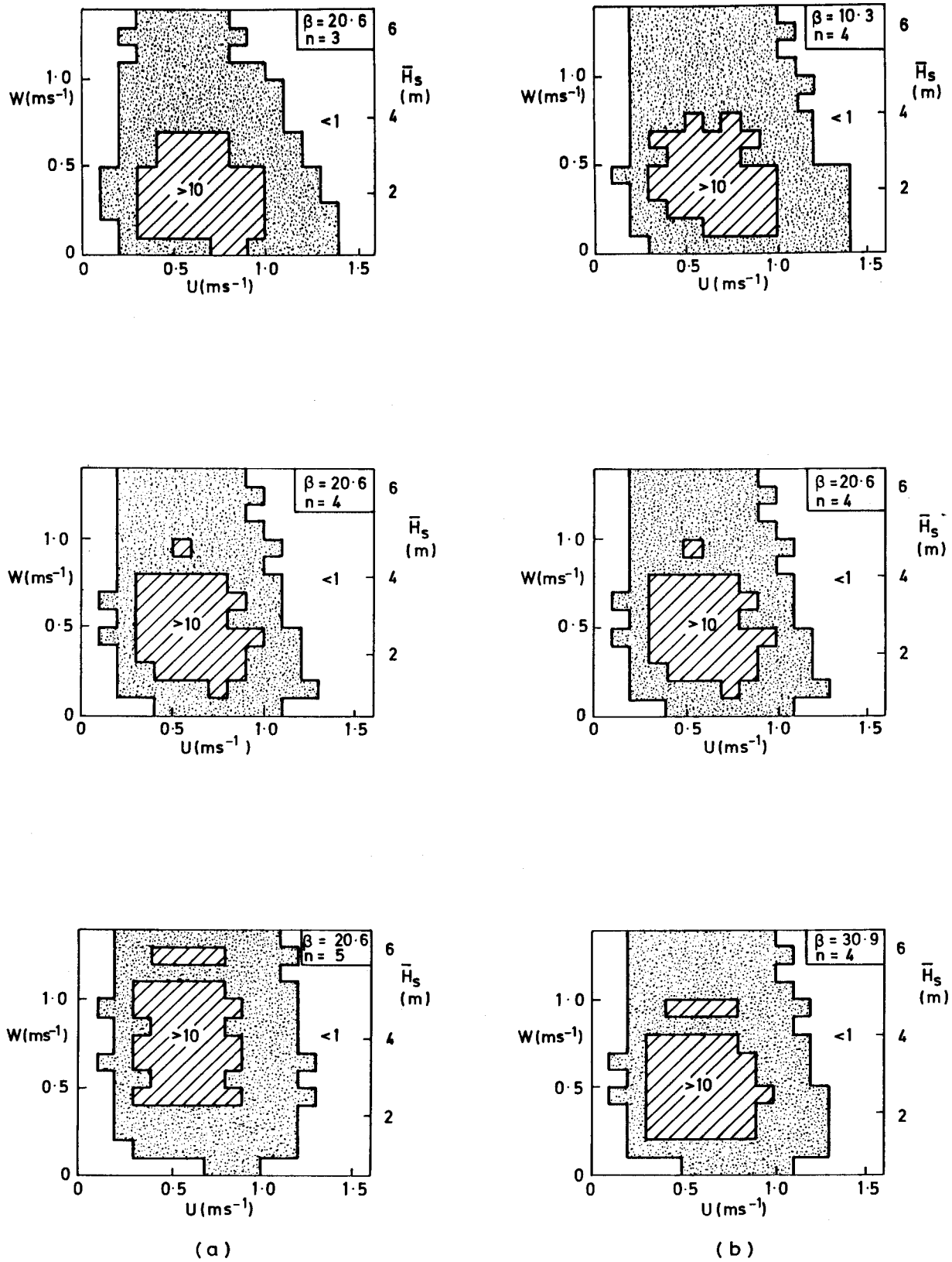

Fig 8 Variation with the constants (a) n and (b) β in Eq (9) of the distribution $S_{cw}(U_i, W_j)$